

Slow Magnetic Relaxation of a 12-Metallacrown-4 Complex with a Manganese(III)-Copper(II) Heterometallic Ring Motif

Alex J. Lewis[†], Elena Garlatti^{§‡}, Francesco Cugini[‡], Massimo Solzi[‡], Matthias Zeller[‡], Stefano Carretta^{§‡}, and Curtis M. Zaleski^{†*}*

[†]Department of Chemistry and Biochemistry, Shippensburg University, Shippensburg, Pennsylvania 17257, United States

[‡]Dipartimento di Scienze Matematiche, Fisiche e Informatiche, Università di Parma, 1-43124 Parma, Italy

[§]Udr Parma, INSTM, 1-43124 Parma, Italy

[‡]Department of Chemistry, Purdue University, West Lafayette, Indiana 47907, United States

ABSTRACT

The heterobimetallic metallacrown (MC), $(\text{TMA})_2\{\text{Mn}(\text{OAc})_2[12\text{-MC}_{\text{Mn}^{\text{III}}\text{Cu}^{\text{II}}(\text{N})\text{shi}^-4](\text{CH}_3\text{OH})\} \cdot 2.90\text{CH}_3\text{OH}$, **1**, where TMA^+ is tetramethylammonium, OAc^- is acetate, and shi^{3-} is salicylhydroximate, consists of a Mn^{II} ion captured in the central cavity and alternating unambiguous and ordered manganese(III) and copper(II) sites about the MC ring, a first for the archetypal MC structure design. DC-magnetometry characterization and subsequent simulation

with the Spin Hamiltonian $\mathcal{H} = -J_1(\mathbf{s}_1 + \mathbf{s}_3) \cdot \mathbf{s}_5 - J_2(\mathbf{s}_2 + \mathbf{s}_4) \cdot \mathbf{s}_5 - J_3 \sum_{i=1}^4 \mathbf{s}_i \cdot \mathbf{s}_{i+1} + d (s_{z,1}^2 + s_{z,3}^2) + \mu_B \sum_{j=1}^5 g_j \mathbf{s}_j \cdot \mathbf{B}$, indicate an $S = 5/2$ ground state and a sizeable axial zero-field splitting on Mn^{III} . AC-susceptibility measurements reveal that **1** displays slow magnetization relaxation akin to single-molecule magnet (SMM) behavior.

TEXT

Metallamacrocyclic compounds such as wheels¹, rings², helicates³, cryptates⁴, calixarenes⁵, coronates⁶, and metallacrowns⁷, provide a great deal of synthetic flexibility for chemists. Indeed, these molecules can be varied by substituting one metal⁸ or ligand⁹ choice for another without changing the overall molecular structure. Thus, the physical properties of a system can be fine-tuned by component choice. The characteristics and properties of these compounds impact a large breath of areas, including metalloenzyme active sites models, luminescence, molecular magnetism, and sensors.¹⁰ In particular, metallacrowns (MCs) have proven to be a versatile class of coordination complexes, from structural and functional analogues of crown ethers to recent examples of bioimaging agents.^{11,12} Furthermore, MCs tend to possess interesting magnetic properties, especially as SMMs.¹²⁻¹⁴ Their wide range of applications is due to their ability to be formed in a predictable fashion based on metal and ligand choice and that the systems can incorporate different metal types in one molecule.

The archetypal MC motif consists of a cyclic ring with a M-N-O repeat unit and the oxygen atoms generate a central cavity, which binds a metal ion. Though the definition of a MC has expanded since the first reports to include molecules such as azametallacrowns, inverse MCs, collapsed MCs, and other larger structures that do not strictly adhere to the M-N-O repeat unit.^{12,13}

While the first MCs tended to be homometallic, chemists quickly devised ways to synthesize heterobimetallic systems and since 2014 heterotrimetallic MCs have become more common.¹⁵ In most heterometallic MC systems, the ring metals are of one type e.g. a transition metal, and the metal ion(s) captured in the central cavity is of a different variety (an alkali and/or lanthanide ion). What is lacking in the field is the use of two or more different 3*d* transition metal ions in an archetypal MC complex. Only one example qualifies as an archetypal MC with more than one 3*d* transition metal: a 12-MC-4 complex with ring Fe^{III} ions and a central Cu^{II} ion.¹⁶ This molecule is though typical of other heterobimetallic systems with segregated sites for the two different metal species.

Herein we report the first archetypal MC, (TMA)₂{Mn(OAc)₂[12-MC_{Mn^{III}Cu^{II}(N)shi-4}](CH₃OH)}·2.90CH₃OH, **1**, to contain two different metal ions in the MC ring with manganese(III) and copper(II) ions in unambiguous coordination sites. This is significant as two different metal ions are often disordered about the coordination sites in other heterometallic macrocycles, such as metallic wheels and rings.^{8,17} By careful choice of ligands and synthetic schemes ordered heterometallic antiferromagnetic rings can be obtained^{9,18}; however, the majority of instances have a disordered metal sites. For the 3*d* heterobimetallic 12-MC_{Mn^{III}Cu^{II}}-4 compound **1**, the manganese(III) and copper(II) ions alternate in a defined, ordered fashion about the ring. Additionally, DC-magnetometry characterization indicates a mixed antiferromagnetic-ferromagnetic exchange between the metals, and AC-magnetic susceptibility measurements suggest SMM-like behavior.

Complex **1** can be prepared by combining salicylhydroxamic acid and tetramethylammonium acetate in methanol followed by the addition of copper(II) acetate and manganese(II) acetate (synthetic details in SI). Complex **1** possesses the traditional metallacrown connectivity with a M-N-O repeat unit about the MC ring, and the Mn^{III}-N-O-Cu^{II}-N-O pattern recurs twice to generate the MC (Figures 1 and S1). The metallacrown captures a Mn^{II} ion in the central cavity akin to the original 12-MC-4: Mn(OAc)₂[12-MC_{Mn^{III}(N)shi-4}](DMF)₆·2DMF, **2**, which contains a central Mn^{II} and only ring Mn^{III} ions.^{11,19} If the expanded definitions of MCs are considered, several heterometallic ring MCs have been reported including collapsed MCs²⁰, inverse MCs²¹, and large MC-like complexes²². However, these structures either lack a central cavity, bind a nonmetal atom in the central cavity, or lack a continuous M-N-O repeat unit, respectively. None of these systems are the archetypal MC with a M-N-O connectivity throughout the molecule and a central metal ion captured in the MC cavity.^{12,13} Thus, **1** represents the only heterometallic ring archetypal MC reported to date. Moreover, the two different ions are ordered about the MC ring unlike many heterometallic ring compounds.^{8,17}

The metal oxidation states are based on average bond lengths, bond valence sum (BVS) values²³, and overall molecular charge balance considerations (Tables S2 and S3). Four triply deprotonated salicylhydroximate ligands and two acetate anions provide a 14- charge, which is counterbalanced by two ring Mn^{III} ions, two ring Cu^{II} ions, one central Mn^{II} ion, and two lattice tetramethylammonium cations (14+ charge). The overall structure of the MC is a square molecule that is slightly domed away from the central Mn^{II} ion. The Mn^{II} (Mn3) is six-coordinate with a coordination sphere comprised of four oxime oxygen atoms from four shi³⁻ ligands, which yield the MC cavity, and two carboxylate oxygen atoms from two acetates. The acetates serve to link the central Mn^{II} to each ring Mn^{III} ion. A SHAPE analysis (*SHAPE 2.1*; Table S4) of the Mn^{II}

geometry yields the lowest continuous shape measure (CShM) for an octahedron; however, the geometry is severely distorted as the CShM value (3.491) is greater than the upper threshold value (3.0) that is considered as an adequate description of the geometry.²⁴

The ordered nature of the Cu^{II} and Mn^{III} ions about the MC ring is likely due to the preferred coordination environment of each ion. Furthermore, BVS values and single-crystal X-ray analysis (details in SI) confirm the unambiguous assignment and ordered nature of the ring metal sites. Both Cu^{II} ions are four-coordinate and possess a square planar geometry (Table S4). The coordination environments of Cu1 and Cu2 are identical and consist of trans-chelate rings. A six-membered chelate ring is formed by the oxime nitrogen and phenolate oxygen atoms of one shi³⁻ and the opposite five-membered chelate ring is formed by the oxime and carboxylate oxygen atoms of another shi³⁻. The two ring Mn^{III} ions possess different coordination environments. Mn1 is six-coordinate and has an octahedral geometry with an elongated Jahn-Teller (JT) axis typical for high-spin d^4 ions (Table S4). The equatorial plane consists of trans five- and six-membered chelate rings, same as the Cu^{II} ions. The axial ligands consist of a carboxylate oxygen atom of a bridging acetate and an oxygen atom from a methanol molecule. Mn2 is five-coordinate and possesses a square pyramidal geometry (Table S4) and the tau (τ) value of 0.103 supports the assignment.²⁵ The basal ligands consist of trans five- and six-membered chelate rings, and the apical ligand is a carboxylate oxygen atom of a bridging acetate.

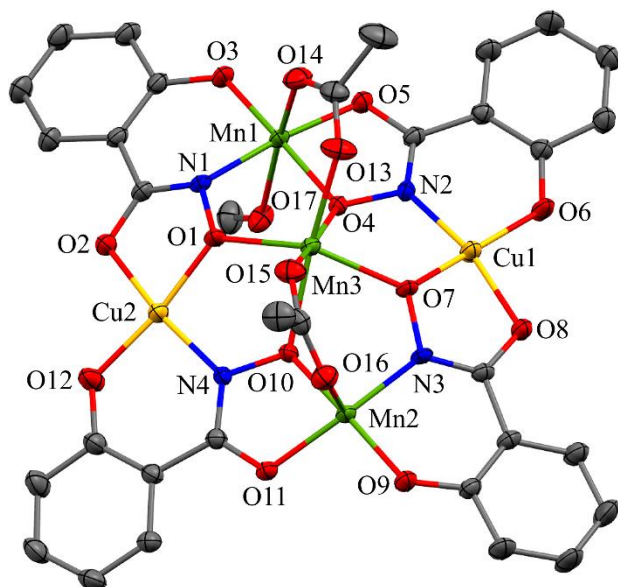


Figure 1. Single-crystal X-ray structure of $(\text{TMA})_2\{\text{Mn}(\text{OAc})_2[12\text{-MC}_{\text{Mn}^{\text{III}}\text{Cu}^{\text{II}}(\text{N})\text{shi}^-4](\text{CH}_3\text{OH})\}\cdot 2.90\text{CH}_3\text{OH}$, **1**. The ellipsoid plot is at the 50% level. Hydrogen atoms, tetramethylammonium cations, and solvent molecules have been omitted for clarity. Color scheme: green, manganese; yellow, copper; red, oxygen; blue, nitrogen; gray, carbon.

Variable-temperature dc magnetic susceptibility measurements of **1** indicate the presence of sizeable antiferromagnetic (AF) interactions (Figure 2). The room temperature χT value ($9.1 \text{ emu K mol}^{-1}$) is less than that expected for the isolated ions ($11.13 \text{ emu K mol}^{-1}$) and decreases with decreasing temperature. The low temperature χT value ($\sim 3.2 \text{ emu K mol}^{-1}$ at 2 K) suggests a total-spin $S = 5/2$ ground state, split by sizeable zero-field splitting (ZFS) effects. The following Spin Hamiltonian can model the magnetic properties of **1**:

$$\mathcal{H} = -J_1(\mathbf{s}_1 + \mathbf{s}_3) \cdot \mathbf{s}_5 - J_2(\mathbf{s}_2 + \mathbf{s}_4) \cdot \mathbf{s}_5 - J_3 \sum_{i=1}^4 \mathbf{s}_i \cdot \mathbf{s}_{i+1} + d(s_{z,1}^2 + s_{z,3}^2) + \mu_B \sum_{j=1}^5 g_j \mathbf{s}_j \cdot \mathbf{B}, \quad (1)$$

(with $s_1 = s_3 = 2$ for Mn^{III} , $s_2 = s_4 = 1/2$ for Cu^{II} , $s_5 = 5/2$ for Mn^{II} and $i + 1 = 1$ for $i = 4$). The first three terms of (1) represent the isotropic Heisenberg exchange interactions (inset Figure 2), the second term is the axial ZFS on the Mn^{III} ions, and the last term accounts for the interaction with the applied magnetic field. The code PHI²⁶ was used to simultaneously fit susceptibility and magnetization data at $T = 2$ K (Figure 3), and two different exchange models, both with axial ZFS on the Mn^{III} ions, were considered: one with two couplings constants (2J model, $J_1 = J_2, J_3$) and another with three couplings constants (3J model, with $J_1 \neq J_2, J_3$).

For the 2J model, the ring $\text{Mn}^{\text{III}}\text{-Cu}^{\text{II}}$ ions have a ferromagnetic (FM) interaction J_3 and they are AF-coupled with the central Mn^{II} . Indeed, $\text{Mn}^{\text{III}}\text{-Cu}^{\text{II}}$ compounds with oxime-based bridging ligands can display FM interactions²⁷, especially in presence of an elongated JT distortion for Mn^{III} as in **1**.²⁸ The number of free parameters can be reduced by setting $|J_{1,2}| = |J_3|$ without affecting the agreement between the data and the simulation of the magnetic susceptibility (Figure 2, red circles) and the magnetization at 2 K (Figure 3, red circles) with $J_1 = J_2 = -12.5 \pm 1.6 \text{ cm}^{-1}$, $J_3 = 12.5 \pm 1.6 \text{ cm}^{-1}$ and $d = -6.5 \pm 1 \text{ cm}^{-1}$. For the simulation, $g_{\text{Mn}^{\text{II}}}$ equaled 2, a typical value for S-ions, and g_{Cu} and $g_{\text{Mn}^{\text{III}}}$ were allowed to vary around typical values²⁹ ($g_{\text{Cu}} = 2.2$ and $g_{\text{Mn}^{\text{III}}} = 1.96$). Energies levels of the exchange and the full Spin Hamiltonian (1) as a function of the magnetic field for the 2J model are found in Figure 4.

With an additional free parameter (3J model) it is possible to improve the agreement with experimental data which leads to two additional sets of best-fit parameters: (1) AF $J_3 = -13.2 \text{ cm}^{-1}$, $J_1 = -7.7 \text{ cm}^{-1}$, $J_2 = -27.1 \text{ cm}^{-1}$ and $d = -6.4 \text{ cm}^{-1}$ (Figures 2 and 3, green triangles) and (2) FM $J_3 = 2.1 \text{ cm}^{-1}$, $J_1 = -6.2 \text{ cm}^{-1}$, $J_2 = -48.6 \text{ cm}^{-1}$ and $d = -7.5 \text{ cm}^{-1}$ (Figures 2 and 3, blue

diamonds). Energies of the total-spin multiplets calculated with the 3J models are reported in Figure S2.

In the model for **1**, only Mn1 and Mn2 have a sizeable single-ion ZFS, within the range of values expected for Mn^{III} ions. To minimize the number of parameters, the same d value was assumed for both, even though they have different coordination geometries. All considered models lead to an axial ZFS parameter d of about -7 cm^{-1} . Additionally, no further improvement of the low-temperature susceptibility or magnetization simulations can be obtained by adding a rhombic term for the ZFS of the Mn^{III} ions or by assuming a small ($\sim 1\text{ cm}^{-1}$) ZFS on Mn^{II}.

Given the available data, the simplest and most reasonable model for **1** is the 2J model, with FM coupling between the ring Mn^{III} and Cu^{II} ions. The 2J model reduces the number of degrees of freedom without significantly affecting the agreement with the data, and the model is supported by previous results that indicate FM couplings between Mn^{III} and Cu^{II} ions mediated by N-O bridges.^{27,28}

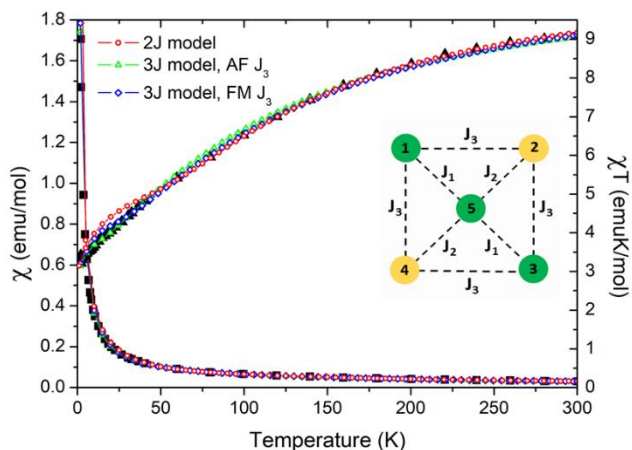


Figure 2. Temperature-dependence of the magnetic susceptibility (χ ; black squares) and χT (black triangles) of **1** ($B = 1000\text{ Oe}$). Line/scatter represent best-fit calculations with the 2J model (red

circles) and the two 3J models (green triangles, blue diamonds). Inset: schematic representation of the exchange couplings.

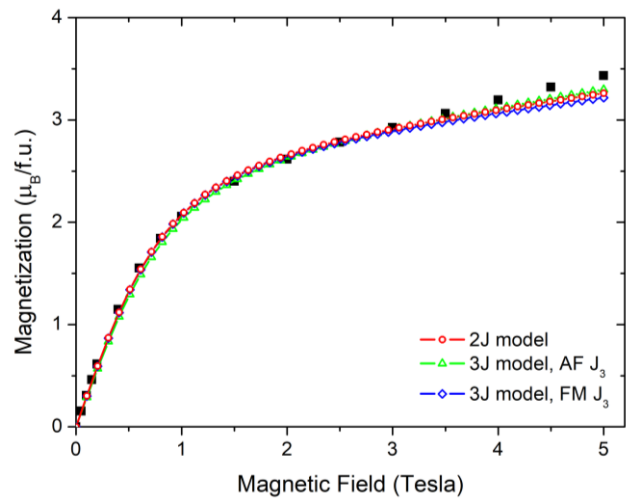


Figure 3. Field-dependence of the magnetization of **1** (squares) at $T = 2$ K. Line/scatter represent the best-fit to the experimental data with the 2J model (red circles) and the two 3J models (green triangles, blue diamonds).

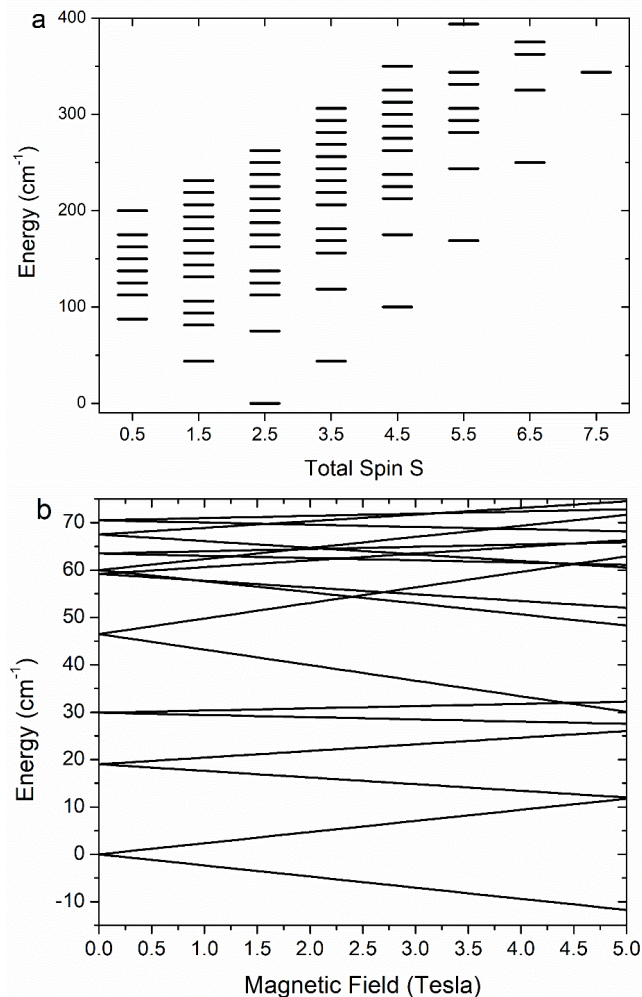


Figure 4. (a) Energy of the total-spin multiplets of **1** calculated with the exchange-only Spin Hamiltonian (S2) and the best-fit constants of the 2J model. The $S = 5/2$ GS energy is set to zero, with degenerate first-excited multiplets $S = 3/2$ and $S = 7/2$. (b) Magnetic field dependence of the lowest lying energy levels calculated with the full Spin Hamiltonian (1) and the 2J model. The magnetic field is applied along the z axis.

The dynamic magnetic behavior of **1** was probed by measuring the AC susceptibility at different frequencies (100 – 1000 Hz) with zero applied dc magnetic field (Figure S3). A frequency-dependent in-phase (χ') signal was observed below 3 K, associated with a frequency-dependent

out-of-phase (χ'') signal. This behavior indicates that **1** possibly behaves as a SMM – similar to **2**.¹⁹ However, for the investigated frequencies χ'' reaches its maximum value below 2 K, outside the experimentally accessible T-range. This is confirmed by the temperature dependence of χ' , which is expected to have an inflection point when χ'' displays a peak. In order to determine the peak position of χ'' at different frequencies and extract the temperature dependence of the relaxation time of **1**, AC measurements below 2 K or as a function of an applied magnetic field³⁰ would be needed. Alternatively, higher frequencies methods like NMR³¹ could be applied. Compared to **2**, complex **1** is characterized by shorter relaxation times at low temperatures thus possessing a lower blocking temperature.¹⁹

In summary, we have synthesized a new heterobimetallic ring MC consisting of ordered metal sites that contains a central metal ion, a first for archetypal metallocrown chemistry. In addition, **1** is only the second 12-MC-4 to consist of two different 3d transition metal ions. The molecule has an $S = 5/2$ GS and a sizeable axial ZFS on the Mn^{III} ions, and the molecule possesses SMM-like behavior. Future studies will focus on synthesizing other metallocrowns with heterometallic rings and understanding how the interaction of the metal ions affects the magnetic properties.

Supporting Information. X-ray crystallographic information of **1** in CIF format. Experimental details, additional crystallographic details and figures, metal-ligand bond distances, BVS values, SHAPE CShM values, spin Hamiltonian and energy levels for **1**, and AC magnetic susceptibility plot (PDF). This material is available free of charge via the Internet at <http://pubs.acs.org>.

Corresponding Author

*Corresponding Authors: stefano.carretta@unipr.it; cmzaleski@ship.edu.

Author Contributions

The manuscript was written through contributions of all authors. All authors have given approval to the final version of the manuscript.

Notes

The authors declare no competing financial interest.

Acknowledgements. E.G. and S.C. gratefully acknowledge financial support from PRIN Project 2015 No. HYFSRT of the Italian MIUR, from the European QuantERA 2017 project SUMO, cofounded by the Italian MUR. E.G. also acknowledges the support of the PRISM Project of the call “FIL-Quota incentivante 2019” of the University of Parma and co-sponsored by Fondazione Cariparma. C.M.Z. and A.J.L. thank the Summer Undergraduate Research Experience (SURE) program, the Faculty Professional Development Council (FPDC) Grant Program, and the Undergraduate Research Program at Shippensburg University for financial support. M.Z. thanks the National Science Foundation for financial support of the single-crystal X-ray diffractometer through the Major Research Instrumentation Program (Grant No. CHE 1625543).

REFERENCES

1. (a) Müller, A.; Krickemeyer, E.; Meyer, J.; Bögge, H.; Peters, F.; Plass, W.; Diemann, E.; Dillinger, S.; Nonnenbruch, F.; Randerath, M.; Menke, C. $[\text{Mo}_{154}(\text{NO})_{14}\text{O}_{420}(\text{OH})_{28}(\text{H}_2\text{O})_{70}]^{(25\pm 5)-}$: A Water-Soluble Big Wheel with More than 700 Atoms and a Relative Mass of About 24000. *Angew. Chem., Int. Ed. Engl.* **1995**, *34*, 2122-2124. (b) Henkelis, J. J.; Jones, L. F.; de Miranda, M. P.; Kilner, C. A.; Halcrow, M. A. Two Heptacopper(II) Disk Complexes with a $[\text{Cu}_7(\mu_3-$

$\text{OH})_4(\mu\text{-OR})_2]^{8+}$ Core. *Inorg. Chem.* **2010**, *49*, 11127-11132. (c) Fraser, H. W. L.; Nichol, G. S.; Baldansuren, A.; McInnes, E. J. L.; Brechin, E. K. Cages on a Plane: A Structural Matrix for Molecular ‘Sheets’. *Dalton Trans.* **2018**, *47*, 15530-15537.

2. (a) Taft, K. L.; Delfs, C. D.; Papaefthymiou, G. C.; Foner, S.; Gatteschi, D.; Lippard, S. L. $[\text{Fe}(\text{OMe})_2(\text{O}_2\text{CCH}_2\text{Cl})]_{10}$, a Molecular Ferric Wheel. *J. Am. Chem. Soc.* **1994**, *116*, 823-832. (b) Murrie, M.; Parsons, S.; Winpenny, R. E. P.; Atkinson, I. M.; Benelli, C. Turing Up the Heat: Synthesis of Octanuclear Chromium(III) Carboxylates. *Chem. Commun.* **1999**, 285-286. (c) Botezat, O.; van Leusen, J.; Kravtsov, V. C.; Kögerler, P.; Baca, S. G. Ultralarge 3d/4f Coordination Wheels: From Carboxylate/Amino Alcohol-Supported $\{\text{Fe}_4\text{Ln}_2\}$ to $\{\text{Fe}_{18}\text{Ln}_6\}$ Rings. *Inorg. Chem.* **2017**, *56*, 1814-1822.

3. (a) Kramer, R.; Lehn, J.-M.; Marquis-Rigault, M. Self-Recognition in Helicate Self-Assembly: Spontaneous Formation of Helical Metal Complexes from Mixture of Ligands and Metal Ions. *Proc. Natl. Acad. Sci. U.S.A.* **1993**, *90*, 5394-5398. (b) Piguet, C.; Bernardinelli, G.; Hopfgartner, G. Helicates as Versatile Supramolecular Complexes. *Chem. Rev.* **1997**, *97*, 2005-2062.

4. (a) Ma, M. S.; Angelici, R. J.; Powell, D.; Jacobson, R. A. Coordination Chemistry of Bis(δ -camphorquinone dioximato)nickel(II) and – palladium(II). Reactions and Structural Studies of Some M_3Ag_2 Cluster Complexes of Camphorquinone Dioxime. *Inorg. Chem.* **1980**, *19*, 3121-3128. (b) Saalfrank, R. W.; Stark, A.; Peters, K.; von Schnering, H. G. The First “Adamantoid”

Alkaline Earth Metal Chelate Complex: Synthesis, Structure, and Reactivity. *Angew. Chem., Int. Ed. Engl.* **1988**, *27*, 851-853.

5. (a) Rauter, H.; Hillgeris, E. C.; Erxleben, A.; Lippert, B. Platinum Complex [(en)Pt(uracilate)]₄⁴⁺: A Metal Analog of Calix[4]arene. Similarities and Differences with Classical Calix[4]arenes. *J. Am. Chem. Soc.* **1994**, *116*, 616-624. (b) Xu, W.; Vittal, J. J.; Puddephatt, R. J. Inorganic Inclusion Chemistry: A Novel Anion Inclusion System. *J. Am. Chem. Soc.* **1995**, *117*, 8362-8371.

6. Saalfrank, R. W.; Bernt, I.; Uller, E.; Hampel, F. Template-Mediated Self Assembly of Six- and Eight-Membered Iron Coronates. *Angew. Chem. Int. Ed. Engl.* **1997**, *36*, 2482-2425.

7. (a) Pecoraro, V. L. Structural Characterization of [VO(salicylhydroximate)(CH₃OH)]₃: Applications to the Biological Chemistry of Vanadium(V). *Inorg. Chim. Acta* **1989**, *155*, 171-173. (b) Pecoraro, V. L.; Stemmler, A. J.; Gibney, B. R.; Bodwin, J. J.; Wang, H.; Kampf, J. W.; Barwinski, A. Metallacrowns: A New Class of Molecular Recognition Agents. In *Progress in Inorganic Chemistry*; Karlin, K. D., Ed.; John Wiley & Sons: New York, **1997**; Vol. 45, pp 83-177.

8. (a) Larsen, F. K.; McInnes, E. J. L.; El Mkami, H.; Overgaard, J.; Piligkos, S.; Rajaraman, G.; Rentschler, E.; Smith, A. A.; Smith, G.; M.; Boote, V.; Jennings, M.; Timco, G. A.; Winpenny, R. E. P. Synthesis and Characterization of Heterometallic $\{\text{Cr}_7\text{M}\}$ Wheels. *Angew. Chem. Int. Ed.* **2003**, *42*, 101-105. (b) Casadei C. M.; Bordonali L.; Furukawa Y.; Borsa F.; Garlatti E.; Lascialfari A.; Carretta S.; Sanna S.; Timco G.; Winpenny R. Local spin density in the Cr_7Ni antiferromagnetic molecular ring and ^{53}Cr -NMR. *J. Phys.: Condens. Matter* **2012**, *24*, 406002. (c) Timco, G. A.; Batsanov, A. S.; Larsen, F. K.; Murn, C. A.; Overgaard, J.; Teat, S. J.; Winpenny, R. E. P. Influencing the Nuclearity and Constitution of Heterometallic Rings via Templates. *Chem. Commun.* **2005**, 3649-3651. (d) Garlatti E.; Guidi T.; Chiesa A.; Ansbro S.; Baker M. L.; Ollivier J.; Mutka H.; Timco G. A.; Vitorica-Yrezabal I.; Pavarini E.; Santini P.; Amoretti G.; Winpenny R. E. P.; Carretta S. Anisotropy of Co^{II} transferred to the Cr_7Co polymetallic cluster via strong exchange interactions. *Chem. Sci.* **2018**, *9*, 3555-3562.

9. (a) Timco, G. A.; McInnes, E. J. L.; Pritchard, R. G.; Tuna, F.; Winpenny, R. E. P. Heterometallic Rings Made From Chromium Stick Together Easily. *Angew. Chem., Int. Ed.* **2008**, *47*, 9681-9684. (b) Garlatti E.; Albring M. A.; Baker M. L.; Docherty R. J.; Mutka H.; Guidi T.; Garcia Sakai V.; Whitehead G. F. S.; Pritchard R. G.; Timco G. A.; Tuna F.; Amoretti G.; Carretta S.; Santini P.; Lorusso G.; Affronte M.; McInnes E. J. L.; Collison D.; Winpenny R. E. P. A Detailed Study of the Magnetism of Chiral $\{\text{Cr}_7\text{M}\}$ Rings: An Investigation into Parametrization and Transferability of Parameters. *J. Am. Chem. Soc.* **2014**, *136*, 9736-9772.

10. (a) Chakrabarty, R.; Mukherjee, P. S.; Stang, P. J. Supramolecular Coordination: Self-Assembly of Finite Two- and Three-Dimensional Ensembles. *Chem. Rev.* **2011**, *111*, 6810-6918. (b) Amouri, H.; Desmarests, C. Moussa, J. Confined Nanospaces in Metallocages: Guest Molecules, Weakly Encapsulated Anions, and Catalyst Sequestration. *Chem. Rev.* **2012**, *112*, 2015-2041. (c) Li, H.; Yao, Z.-J.; Yao; Liu, D.; Jin, G.-X. Multi-Component Coordination-Drive Self-Assembly Toward Heterometallic Macrocycles and Cages. *Coord. Chem. Rev.* **2015**, *293-294*, 139-157. (d) Gorczyński, A.; Harrowfield, J. M.; Patroniak, V.; Stefankiewicz, A. R. Quarterpyridines as Scaffolds for Functional Metallosupramolecular Materials. *Chem. Rev.* **2016**, *116*, 14620-14674. (e) Zhang, Y.-Y.; Gao, W.-X.; Jin, G.-X. Recent Advances in the Construction and Applications of Heterometallic Macrocycles and Cages. *Coord. Chem. Rev.* **2017**, *344*, 323-344.

11. Lah, M. S.; Pecoraro, V. L. Isolation and Characterization of $\{\text{Mn}^{\text{II}}[\text{Mn}^{\text{III}}(\text{salicylhydroximate})_4(\text{acetate})_2(\text{DMF})_6]\cdot 2\text{DMF}\}$: An Inorganic Analogue to $\text{M}^{2+}(12\text{-crown-4})$. *J. Am. Chem. Soc.* **1989**, *111*, 7258-7259.

12. (a) Chow, C. Y.; Trivedi, E. R.; Pecoraro, V.; Zaleski, C. M. Heterometallic Mixed 3d-4f Metallocrowns: Structural Versatility, Molecular Magnetism, and Luminescence. *Comments Inorg. Chem.* **2015**, *35*, 214-253. (b) Ostrowska, M.; Fritsky, I. O.; Gumienna-Kontecka, E.; Pavlishchuk, A. V. Metallocrown-based Compounds: Applications in Catalysis, Luminescence, Molecular Magnetism, and Adsorption. *Coord. Chem. Rev.* **2016**, *327-328*, 304-332. (c) Nguyen, T. N.; Pecoraro, V. L. Metallocrowns: From Discovery to Potential Applications in Biomolecular

Imaging. In *Comprehensive Supramolecular Chemistry II*; Atwood, J. L., Ed.; Elsevier: Oxford, UK, **2017**; Vol 5, pp 195-212. (d) Lutter, J. C.; Zaleski, C. M.; Pecoraro, V. L. Metallacrowns: Supramolecular Constructs with Potential in Extended Solids, Solution-State Dynamics, Molecular Magnetism, and Imaging. In *Advances in Inorganic Chemistry*; van Eldik, R. and Puchta, R., Eds.; Academic Press: Cambridge, MA, **2018**; Vol. 71, pp 177-246.

13. (a) Mezei, G.; Zaleski, C. M.; Pecoraro, V. L. Structural and Functional Evolution of Metallacrowns. *Chem. Rev.* **2007**, *107*, 4933-5003. (b) Lah, M. S.; John, R. P.; Moon, D. Metalladiazamacrocycles: Metallamacrocycles as Potential Supramolecular Host System for Small Organic Guest Molecules and Supramolecular Building Blocks for Metal Organic Frameworks. *Supramol. Chem.* **2007**, *19*, 295-308. (c) Tegoni, M.; Remelli, M. Metallacrowns of Copper(II) and Aminohydroxamates: Thermodynamics of Self Assembly and Host-Guest Equilibria. *Coord. Chem. Rev.* **2012**, *256*, 289-315. (d) Pavlishchuk, A. V.; Satska, Y. A.; Kolotilov, S. V.; Fritsky, I. O. Coordination Polymers and Oligonuclear Systems Based on Oximate or Hydroxamate Building Blocks: Magnetic and Sorption Properties. *Curr. Inorg. Chem.* **2015**, *5*, 5-25.

14. (a) Dendrinou-Samara, C.; Alexiou, M.; Zaleski, C. M.; Kampf, J. W.; Kirk, M. L.; Kessissoglou, D. P.; Pecoraro, V. L. Synthesis and Magnetic Properties of a Metallacryptate that Behaves as a Single-Molecule Magnet. *Angew. Chem. Int. Ed.* **2003**, *42*, 3763-3766. (b) Zaleski, C. M.; Depperman, E. C.; Dendrinou-Samara, C., Alexiou, M.; Kampf, J. W.; Kessissoglou, D. P.; Kirk, M. L.; Pecoraro, V. L. Metallacryptate Single-Molecule Magnets: The Effect of Lower

Molecular Symmetry on Blocking Temperature. *J. Am. Chem. Soc.* **2005**, *127*, 12862-12872. (c) Zaleski, C. M.; Depperman, E. C.; Kampf, J. W.; Kirk, M. L.; Pecoraro, V. L. Using $\text{Ln}^{\text{III}}[\text{15-MC}_{\text{Cu}^{\text{II}}(\text{N})(\text{S})\text{-pheHA-5}}]^{3+}$ Complexes to Construct Chiral Single-Molecule Magnets and Chains of Single-Molecule Magnets. *Inorg. Chem.* **2006**, *45*, 10022-10024. (d) Cao, F.; Wei, R.-M.; Li, J.; Yang, L.; Han, Y.; Song, Y.; Dou, J.-M. Ferromagnetic Polarization: The Quantum Picture of Switching On/Off Single-Molecule Magnetism. *Inorg. Chem.* **2016**, *55*, 5914-5923. (e) Boron, T. T., III; Lutter, J. C.; Daly, C. I.; Chow, C. Y.; Davis, A. H.; Nimthong-Roldán, A.; Zeller, M.; Kampf, J. W.; Zaleski, C. M.; Pecoraro, V. L. The Nature of the Bridging Anion Controls the Single-Molecule Magnetic Properties of DyX_4M 12-Metallacrown-4 Complexes. *Inorg. Chem.* **2016**, *55*, 10597-10607. (f) Yang, W.; Yang, H.; Zeng, S.-Y.; Li, D.-C.; Dou, J.-M. Unprecedented Family of Heterometallic $\text{Ln}^{\text{III}}[\text{18-metallacrown-6}]$ Complexes: Syntheses, Structures, and Magnetic Properties. *Dalton Trans.* **2017**, *46*, 13027-13034. (g) Wang, J.; Ruan, Z.-Y.; Li, Q.-W.; Chen, Y.-C.; Huang, G.-Z.; Liu, J.-L.; Reta, D.; Chilton, N. F.; Wang, Z.-X.; Tong, M.-L. Slow Magnetic Relaxation in a $\{\text{EuCu}_5\}$ Metallacrown. *Dalton Trans.* **2019**, *48*, 1686-1692.

15. (a) Azar, M. R.; Boron, T. T., III; Lutter, J. C.; Daly, C. I.; Zegalia, K. A.; Nimthong, R.; Ferrence, G. M.; Zeller, M.; Kampf, J. W.; Pecoraro, V. L.; Zaleski, C. M. Controllable Formation of Heterotrimetallic Coordination Compounds – Systematically Incorporating Lanthanide and Alkali Metal Ions into the Manganese 12-Metallacrown-4 Framework. *Inorg. Chem.* **2014**, *53*, 1729-1742. (b) Travis, J. R.; Zeller, M.; Zaleski, C. M. Facile Carboxylate Ligand Variation of Heterotrimetallic 12-Metallacrown-4 Complexes. *Polyhedron* **2016**, *114*, 29-36. (c) Travis, J. R.; Zeller, M.; Zaleski, C. M. Crystal structure of tetraaqua(dimethylformamide) tetrakis(1-N,2-

dioxidobenzene-1-carboximidato)tetrakis(1-trimethylacetato)tetramanganese(III)sodiumyttrium–dimethylformamide–water (1/8.04/0.62). *Acta Cryst.* **2015**, *E71*, 1300-1306.

16. Happ, P.; Rentschler, E. Enforcement of a High-Spin Ground State for the First 3d Heterometallic 12-Metallacrown-4 Complex. *Dalton Trans.* **2014**, *43*, 15308-15312.

17. (a) McInnes, E. J. L.; Timco, G. A.; Whitehead, G. F. S.; Winpenny, R. E. P. Heterometallic Rings: Their Physics and Use as Supramolecular Building Blocks. *Angew. Chem. Int. Ed.* **2015**, *54*, 14244-14269. (b) Kobayashi, F.; Ohtani, R.; Kusumoto, S.; Lindoy, L. F.; Hayami, S.; Nakamura, M. Wheel-Type Heterometallic Ferromagnetic Clusters: $[\text{Ni}_{7-x}\text{M}_x(\text{HL})_6(\mu_3\text{-OH})_2]\text{Cl}_2$ ($\text{M} = \text{Zn}, \text{Co}, \text{Mn}$; $X = 1, 3$). *Dalton Trans.* **2018**, *47*, 16422-16428. (c) Fraser, H. W. L.; Nichol, G. S.; Uhrin, D.; Nielsen, U. G.; Evangelisti, M.; Schnack, J.; Brechin, E. K. Order in Disorder: Solution and Solid-State Studies of $[\text{M}^{\text{III}}_2\text{M}^{\text{II}}_5]$ Wheels ($\text{M}^{\text{III}} = \text{Cr}, \text{Al}$; $\text{M}^{\text{II}} = \text{Ni}, \text{Zn}$). *Dalton Trans.* **2018**, *47*, 11834-11842.

18. (a) Larsen, F. K. Overgaard, J.; Parson, S.; Rentschler, E.; Smith, A. A. Timco, G. A.; Winpenny, R. E. P. Horseshoes, Rings, and Distorted Rings: Studies of Cyclic Chromium-Fluoride Cages. *Angew. Chem. Int. Ed.* **2003**, *42*, 5978-5981. (b) Timco, G.; Marocchi, S.; Garlatti, E.; Barker, C.; Albring, M.; Bellini, V.; Manghi, F.; McInnes, E. J. L.; Pritchard, R. G.; Tuna, F.; Wernsdorfer, W.; Lorusso, G.; Amoretti, G.; Carretta, S.; Affronte, M.; Winpenny, R. E. P. Heterodimers of Heterometallic Rings. *Dalton Trans.* **2016**, *45*, 16610-16615.

19. Zaleski, C. M.; Tricard, S.; Depperman, E. C.; Wernsdorfer, W.; Mallah, T.; Kirk, M. L.; Pecoraro, V. L. Single Molecule Magnet Behavior of a Pentanuclear Mn-Based Metallocrown Complex: Solid State and Solution Magnetic Studies. *Inorg. Chem.* **2011**, *50*, 11348-11352.

20. (a) Psomas, G.; Stemmler, A. J.; Dendrinou-Samara, C.; Bodwin, J. J.; Schneider, M.; Alexiou, M.; Kampf, J. W.; Kessissoglou, D. P.; Pecoraro, V. L. Preparation of Site-Differentiated Mixed Ligand and Mixed Ligand/Mixed Metal Metallocrowns. *Inorg. Chem.* **2001**, *40*, 1562-1570. (b) Alaimo, A.; Alexandropoulos, D. I.; Lampropoulos, C.; Stamatatos, T. C. New Insights in Mn-Ca Chemistry from the Use of Oximate-Based Ligands: $\{\text{Mn}^{\text{II/III}}_{22}\text{Ca}_2\}$ and $\{\text{Mn}^{\text{IV}}_2\text{Ca}_2\}$ Complexes with Relevance to Both Low- and High-Valent States of the Oxygen-Evolving Complex. *Polyhedron* **2018**, *149*, 39-44. (c) Gole, B.; Chakrabarty, R.; Mukherjee, S.; Song, Y.; Mukherjee, P. S. Use of 2-pyrimidineamidoxime to Generate Polynuclear Homo-/Heterometallic Assemblies: Synthesis, Crystal Structures, and Magnetic Study with Theoretical Investigations on the Exchange Mechanism. *Dalton. Trans.* **2010**, *39*, 9766-9778. (d) Hołyńska, M.; Korabik, M. Preparation and Properties of a Series of $[\text{Cr}_2\text{Ln}_2]$ Oximate-Bridged Complexes. *Eur. J. Inorg. Chem.* **2013**, *2013*, 5469-5475. (e) Papatriantafyllopoulou, C.; Estrader, M.; Efthymiou, C. G.; Dermizaki, D.; Gkotsis, K.; Terzis, A.; Diaz, C.; Perlepes, S. P. In Search for Mixed Transition Metal/Lanthanide Single-Molecule Magnets: Synthetic Routes to $\text{Ni}^{\text{II}}/\text{Tb}^{\text{III}}$ and $\text{Ni}^{\text{II}}/\text{Dy}^{\text{III}}$ Clusters Featuring a 2-Pyridyl Oximate Ligand. *Polyhedron* **2009**, *28*, 1652-1655.

21. (a) Chesman, A. S. R.; Turner, D. R.; Berry, K. J.; Chilton, N. F.; Moubaraki, B.; Murray, K. S.; Deacon, G. B.; Batten, S. R. $\text{Ln}^{\text{III}}_2\text{Mn}^{\text{III}}_2$ Heterobimetallic “Butterfly” Complexes Displaying Antiferromagnetic Coupling (Ln = Eu, Gd, Tb, Er). *Dalton Trans.* **2012**, *41*, 11402-11412. (b)

Shiga, T.; Maruyama, K.; Newton, G. N. Inglis, R.; Brechin, E. K.; Oshio, H. Chiral Single-Chain Magnet: Helically Stacked $[\text{Mn}^{\text{III}}_2\text{Cu}^{\text{II}}]$ Triangles. *Inorg. Chem.* **2014**, *53*, 4272-4274. (c) Nesterova, O. V.; Chygorin, E. N.; Kokozay, V. N.; Omelchenko, I. V.; Shishkin, O. V.; Boča, R.; Pombeiro, A. J. L. A Self-Assembled Octanuclear Complex Bearing the Uncommon Close-Packed $\{\text{Fe}_4\text{Mn}_4(\mu_4\text{-O})_4(\mu\text{-O})_4\}$ Molecular Core. *Dalton Trans.* **2015**, *44*, 14918-14924. (d) Yang, H.; Cao, F.; Li, D.; Zeng, S.; Song, Y.; Dou, J. A Family of 12-Azametallacrown-4 Structural Motif with Heterometallic $\text{Mn}^{\text{III}}\text{-Ln-Mn}^{\text{III}}\text{-Ln}$ ($\text{Ln} = \text{Dy, Er, Yb, Tb, Y}$) Alternate Arrangement and Single-Molecule Magnet Behavior. *Chem. Eur. J.* **2015**, *21*, 14478-14485.

22. (a) Zaleski, C. M.; Depperman, E. C.; Kampf, J. W.; Kirk, M. L.; Pecoraro, V. L. Synthesis, Structure, and Magnetic Properties of a Large Lanthanide – Transition Metal Single-Molecule Magnet. *Angew. Chem. Int. Ed.* **2004**, *43*, 3911-3914. (b) Zaleski, C. M.; Kampf, J. W.; Mallah, T.; Kirk, M. L.; Pecoraro, V. L. Assessing the Slow Magnetic Relaxation Behavior of $\text{Ln}^{\text{III}}_4\text{Mn}^{\text{III}}_6$ Metallacrowns. *Inorg. Chem.* **2007**, *46*, 1954-1956. (c) Chow, C. Y.; Bolvin, H.; Campbell, V. E.; Guillot, R.; Kampf, J. W.; Wernsdorfer, W.; Gendron, F.; Autschbach, J.; Pecoraro, V. L. Mallah, T. Assessing the Exchange Coupling in Binuclear Lanthanide(III) Complexes and the Slow Relaxation of the Magnetization in the Antiferromagnetically Coupled Dy_2 Derivative. *Chem. Sci.* **2015**, *6*, 4148-4159. (d) Zhang, H.-G.; Du, Y.-C.; Yang, H.; Zhuang, M.-Y.; Li, D.-C.; Dou, J.-M. A New Family of $\{\text{Co}_4\text{Ln}_8\}$ Metallacrowns with a Butterfly-Shaped Structure. *Inorg. Chem. Front.* **2019**, *6*, 1904-1908. (e) Jankolovits, J.; Kampf, J. W.; Pecoraro, V. L. Solvent Dependent Assembly of Lanthanide Metallacrowns Using Building Blocks with Incompatible Symmetry Preferences. *Inorg. Chem.* **2014**, *53*, 7534-7546. (f) Dong, H.-M.; Liu, Z.-Y.; Yang, E.-C.; Zhao, X.-J. A Novel Oxime-Derived 3d-4f Single-Molecule Magnet Exhibiting Two

Single-Ion Magnetic Relaxations. *Dalton Trans.* **2016**, *45*, 11876-11882. (g) Dong, H.-M.; Zhang, Z.-C.; Li, H.-Y.; Liu, Z.-Y.; Yang, E.-C.; Zhao, X.-J. High-Nuclear Heterometallic Oxime Clusters Assembled from Triangular Subunits: Solvothermal Syntheses, Crystal Structures and Magnetic Properties. *Dalton Trans.* **2018**, *47*, 169-179. (h) Cao, F.; Wang, S.; Li, D.; Zeng, S.; Niu, M.; Song, Y.; Dou, J. Family of Mixed 3d-4f Dimeric 14-Metallacrown-5 Compounds: Syntheses, Structures, and Magnetic Properties. *Inorg. Chem.* **2013**, *52*, 10747-10755. (i) Deb, A.; Boron, T. T., III; Itou, M.; Sakurai, Y.; Mallah, T.; Pecoraro, V. L.; Penner-Hahn, J. E. Understanding Spin Structure in Metallacrown Single-Molecule Magnets using Magnetic Compton Scattering. *J. Am. Chem. Soc.* **2014**, *136*, 4889-4892. (j) Boron, T. T., III; Kampf, J. W.; Pecoraro, V. L. A Mixed 3d-4f 14-Metallacrown-5 Complex that Displays Slow Magnetic Relaxation through Geometric Control of Magnetoanisotropy. *Inorg. Chem.* **2010**, *49*, 9104-9106.

23. Liu, W.; Thorp, H. H. Bond Valence Sum Analysis of Metal-Ligand Bond Lengths in Metalloenzymes and Model Complexes. 2. Refined Distances and Other Enzymes. *Inorg. Chem.* **1993**, *32*, 4102-4105.

24. (a) Llunell, M.; Casanova, D.; Cirera, J.; Alemany, P.; Alvarez, S. *SHAPE*, version 2.1; Barcelona, Spain, 2013. (b) Pinksy, M.; Avnir, D. Continuous Symmetry Measures. 5. The Classical Polyhedra. *Inorg. Chem.* **1998**, *37*, 5575-5582. (c) Casanova, D.; Cirera, J.; Llunell, M.; Alemany, P.; Avnir, D.; Alvarez, S. Minimal Distortion Pathways in Polyhedral Rearrangements. *J. Am. Chem. Soc.* **2004**, *126*, 1755-1763. (d) Cirera, J.; Ruiz, E.; Alvarez, S. Continuous Shape

Measures as a Stereochemical Tool in Organometallic Chemistry. *Organometallics* **2005**, *24*, 1556-1562.

25. Addison, A. W.; Rao, T. N.; Reedijk, J.; van Rijn, J.; Verschoor, G. C. Synthesis, Structure, and Spectroscopic Properties of Copper(II) Compounds Containing Nitrogen–Sulphur donor Ligands; The Crystal and Molecular Structure of Aqua[1,7-bis(*N*-methylbenzimidazol-2'-yl)-2,6-dithiaheptane]copper(II) Perchlorate. *J. Chem. Soc., Dalton Trans.* **1984**, *7*, 1349-1356.

26. Chilton, N. F.; Anderson, R. P.; Turner, L. D.; Soncini, A.; Murray, K. S. PHI: a powerful new program for the analysis of anisotropic monomeric and exchange-coupled polynuclear d- and f-block complexes, *J. Comput. Chem.* **2013**, *34*, 1164-1175.

27. (a) Lloret, F.; Ruiz, R.; Julve, M.; Faus, J.; Journaux, Y.; Castro, I.; Verdaguer, M. metamagnetic properties of a family of ferromagnetic alternating spin chains: Bis(dimethylglyoximato)(carboxylato)manganese(III)copper(II) *Chem. Mater.* **1992**, *4*, 1150-1153. (b) Birkelbach, F.; Winter, M.; Florke, U.; Haupt, H.-J.; Butzlaff, C.; Lengen, M.; Bill, E.; Trautwein, A. X.; Wieghardt, K.; Chaudhuri, P. Exchange Coupling in Homo- and Heterodinuclear Complexes CuM [M = Cr(III), Mn(III), Mn(II), Fe(III), Co(III), Co(II), Ni(II), Cu(II), Zn(II)]. Synthesis, structures, and spectroscopic properties *Inorg. Chem.* **1994**, *33*, 3990-4001.

28. (a) Oshio, H.; Nihei, M.; Yoshida, A.; Nojiri, H.; Nakano, M.; Yamaguchi, A.; Karaki, Y.; Ishimoto, H. A Dinuclear Mn^{III}–Cu^{II} Single-Molecule Magnet *Chem. Eur. J.* **2005**, *11*, 843-848.

(b) Nihei, M.; Yoshida, A.; Koizumi, S.; Oshio, H. Hetero-metal Mn–Cu and Mn–Ni clusters with tridentate Schiff-base ligands *Polyhedron* **2007**, *26*, 1997-2007.

29. Mabbs, F. E.; Collison, D. *Electron paramagnetic resonance of d transition metal compounds; Studies in Inorganic Chemistry*; Elsevier Science: Amsterdam, 1992; Vol. 16.

30. (a) Luis, F.; Bartolomé, J.; Fernández, J. F.; Tejada, J.; Hernández, J. M.; Zhang, X. X.; Ziolo, R. Thermally activated and field-tuned tunneling in Mn₁₂Ac studied by ac magnetic susceptibility. *Phys. Rev. B* **1997**, *55*, 11448-11456. (b) Garlatti, E.; Carretta, S.; Affronte, M.; Sañudo, E. C.; Amoretti, G.; Santini, P. Magnetic properties and relaxation dynamics of a frustrated Ni₇ molecular nanomagnet. *J. Phys.: Condens. Matter* **2012**, *24*, 104006. (c) Lutter, J. C.; Eliseeva, S. V.; Kampf, J. W.; Petoud, S.; Pecoraro, V. L. A Unique Ln^{III}{[3.3.1]Ga^{III} Metallacryptate} Series that possesses properties of slow magnetic relaxation and visible/near-infrared luminescence. *Chem. Eur. J.* **2018**, *24*, 10773-10783. (d) Jiang, X.-F.; Chen, M.-G.; Tong, J.-P.; Shao F. A mononuclear dysprosium(III) single-molecule magnet with a non-planar metallacrown. *New J. Chem.* **2019**, *43*, 8704-8710.

31. (a) Garlatti, E., Carretta, S.; Santini, P.; Amoretti, G.; Mariani, M.; Lascialfari, A.; Sanna, S.; Mason, K.; Chang, J.; Tasker, P.; Brechin E. K. Relaxation dynamics in a Fe₇ nanomagnet. *Phys. Rev. B* **2013**, *87*, 054409. (b) Garlatti, E.; Bordignon, S.; Carretta, S.; Allodi, G.; Amoretti, G.; De Renzi, R.; Lascialfari, A.; Furukawa, Y.; Timco, G. A.; Woolfson, R.; Winpenny, R. E. P.; Santini, P. Relaxation dynamics in the frustrated Cr₉ antiferromagnetic ring probed by NMR. *Phys. Rev. B* **2016**, *93*, 024424.

SYNOPSIS

The heterometallic metallacrown (MC), $(\text{TMA})_2\{\text{Mn}(\text{OAc})_2[12\text{-MC}_{\text{Mn}^{\text{III}}\text{Cu}^{\text{II}}(\text{N})\text{shi}^-4](\text{CH}_3\text{OH})\} \cdot 2.90\text{CH}_3\text{OH}$, where TMA^+ is tetramethylammonium, OAc^- is acetate, and shi^{3-} is salicylhydroximate, consists of alternating ring manganese(III) and copper(II) sites and a Mn^{II} ion captured in the central cavity. DC-magnetometry characterization indicate ferromagnetic exchange between the ring metal ions, which then antiferromagnetically couple with the central Mn^{II} ion. AC-susceptibility measurements reveal that metallacrown displays slow magnetization relaxation akin to single-molecule magnet behavior.

